Preprints.org

Synthesis and Characterization of Silica Obtained by Combined Acid-Alkali Treatment of Serpentinite

Abdrazakh Auyeshov , Kazhymuhan Arynov , Chayzada Yeskibayeva [*] , Aytkul Ibraeva , Elmira Dzholdasova

Article

Synthesis and Characterization of Silica Obtained by Combined Acid-Alkali Treatment of Serpentinite

Abdrazakh Aueshov [1], Kazhymukhan Arynov [2], Chayzada Yeskibayeva [1,*], Aytkul Ibrayeva [1] and Elmira Dzholdasova [1]

[1] M. Auezov South Kazakhstan University, 160012, Tauke-Khan St. 5, Shymkent, Kazakhstan

[2] LLP "Institute of Innovative Research and Technology", 050010, 8th Microdistrict, Building 28, Apt. 2, Almaty, Kazakhstan

* Correspondence: centersapa@mail.ru

Abstract

Serpentinite rocks and their processing waste represent a valuable source of magnesium and silicon; however, their complex composition complicates efficient component recovery. This study investigates the combined acid–alkali processing of serpentinite waste from the Zhitikara deposit (Kazakhstan). In the acid leaching stage, sulfuric acid enables magnesium extraction, while subsequent treatment with sodium hydroxide facilitates the selective recovery of silica gel formed during acid attack. At the final neutralization step, amorphous silica is precipitated with a yield exceeding 60% of its initial content. The resulting silica was characterized using FTIR spectroscopy, scanning electron microscopy (SEM–EDS), and BET adsorption analysis. According to IUPAC classification, the obtained material corresponds to mesoporous silica gel with a high specific surface area, suitable for adsorption and catalytic applications. It was shown that the dissolution process follows the shrinking core model. The combined acid–alkali method thus offers a promising approach for processing magnesium hydrosilicates from serpentinite.

Keywords: serpentinite; acid–alkali processing; amorphous silica; industrial waste utilization; shrinking core model; magnesium hydrosilicates

1. Introduction

Serpentinite rocks and their processing waste represent a valuable source of magnesium (up to 43 wt.% MgO) and silica (up to 45 wt.% SiO_2). They have long attracted the attention of researchers as a potential raw material for the production of industrially important magnesium- and silica-based compounds. However, despite extensive research into the integrated processing of serpentinite, practical implementation remains limited. This is primarily due to both technological and economic constraints that hinder the development and application of efficient recovery methods.

From a technological perspective, the challenge lies in the structural and chemical complexity of serpentinite. These rocks are mainly composed of minerals from the serpentine group—such as chrysotile, antigorite, and lizardite—with the general formula $Mg_3Si_2O_5(OH)_4$ or $[Mg(OH)_2(MgOH)_2Si_2O_5]$. While the magnesium-bearing phases are readily soluble in acids, they are unreactive in alkaline media. Consequently, most research has focused on acid-based leaching methods [1–6]. However, although these methods offer certain advantages, they also present serious limitations from both technological and environmental standpoints.

One of the major issues associated with acid leaching (e.g., using H_2SO_4, HCl, or HNO_3) is the formation of insoluble polysilicic acids [7], which convert into hydrated silica gel ($SiO_2 \cdot nH_2O$) during the leaching process. This gel layer forms on the surface of the particles, impeding further dissolution, complicating solid–liquid separation, and reducing the extraction efficiency of magnesium. In

particular, it severely affects filtration and the removal of impurity metals from the pregnant solutions.

To mitigate these issues, it has been proposed to use sub-stoichiometric acid concentrations (30–40% of the theoretical H_2SO_4 requirement). Under such conditions, the quantity of silica gel formed is insufficient to block the surface completely. This approach allows for more efficient acid utilization (up to 98–100%) and achieves magnesium extraction yields of 30–40% [8].

When higher acid concentrations are employed, the resulting dense silica residues can be further processed by alkaline treatment to selectively extract silicon in the form of soluble silicates. This forms the basis of a combined acid–alkali treatment, which enables the concurrent recovery of both magnesium and silicon while reducing secondary waste.

A review of the literature reveals that studies on the combined acid–alkali treatment of serpentinite are fragmented and remain an underexplored research area. According to a recent study by Rakhuba et al. (2023) [4], this method can be successfully applied to technogenic serpentinite waste to produce products suitable for agricultural and construction purposes. Such research is particularly relevant to Kazakhstan, which possesses significant serpentinite reserves and large volumes of chrysotile-asbestos processing waste, as well as extensive areas of low-fertility land. The development of effective methods for utilizing these wastes is of environmental and socioeconomic importance.

The aim of this study is to investigate the processes involved in the combined acid–alkali treatment of serpentinite waste from the Zhitikara deposit (Republic of Kazakhstan). The work includes experimental research in combination with physicochemical methods to examine the dissolution mechanism of layered magnesium hydrosilicates in acid, as well as the structural and adsorption properties of the resulting amorphous silica.

2. Materials and Methods

Serpentinite waste from the Zhitikara deposit (Kazakhstan) with a particle size of ≤0.14 mm was used as the research material. The elemental composition of the sample was (wt.%): Mg – 25.0; Si – 17.45; Fe – 2.93; Al – 0.54; Ca – 0.50.

X-ray diffraction (XRD) patterns were obtained using a D8 Advance diffractometer (Bruker, Germany) equipped with Cu-Kα radiation at 40 kV and 40 mA. The diffraction data were processed using the EVA software package. Phase identification was carried out using the Search/Match function based on the PDF-2 Powder Diffraction File (ICDD).

Fourier-transform infrared (FTIR) spectra were recorded on a Shimadzu IR Prestige-21 spectrometer (Japan) using an ATR (attenuated total reflectance) Miracle accessory by Pike Technologies (USA).

The specific surface area and pore size distribution were determined using the static capacity method (Model: BSD-660S A3) with a degassing zone followed by a temperature-controlled adsorption measurement (Zone-Test: Degas → Temp Zone).

Analytical procedures aimed at determining the elemental distribution during the leaching and purification processes were performed using a JSM-6490LV scanning electron microscope (JEOL, Japan) equipped with an INCA Energy 350 energy-dispersive X-ray spectroscopy (EDS) system.

Theoretical assumptions underlying the experimental investigation of the combined acid–alkali leaching of serpentinite were as follows:

– The mechanism and kinetics of the dissolution of layered magnesium hydrosilicates [9] are described by the shrinking core model and the pseudo-kinetic equation:

$$X = 1 - kt,$$

where: X is the degree of dissolution, k is the reaction rate constant, and t is the time. At the initial stage, the process is controlled by chemical interaction at the surface, while in later stages it becomes limited by the diffusion of the reagent into the porous particle interior.

– Sodium hydroxide (NaOH) dissolves amorphous forms of silica formed during acid treatment, converting them into soluble silicates. Under these conditions, magnesium is only weakly leached from the alkaline medium, enabling the selective extraction of silicon.

For clarity of presentation, the experimental procedures for investigating the acid–alkali treatment of serpentinite are included in the "Results and Discussion" section.

3. Results and Discussion

The combined method involving acid and alkali treatment is based on sequential processes occurring during the dissolution of serpentinite in acid and subsequent treatment of the acid-insoluble residues in alkaline media:

– During the acid leaching stage, the destruction of the crystalline lattice of serpentinite occurs, particularly in the regions of Mg–OH bonds and partially in Si–O–Mg bonds:

$$Mg(OH)_2(MgOH)_2Si_2O_5 + 6H^+ \rightarrow 3Mg^{2+} + 2SiO_2 + 5H_2O \tag{1}$$
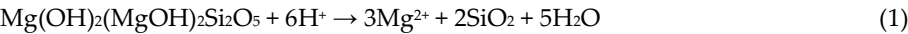
Mg^{2+} ions enter the solution, while the formed amorphous silica ($SiO_2 \cdot nH_2O$) creates a gel-like phase, which causes technological complications during the filtration and purification stages.

– The amorphous $SiO_2 \cdot nH_2O$ reacts well with alkalis, transforming into soluble silicates.

$$SiO_2 \cdot nH_2O + 2NaOH \rightarrow Na_2SiO_3 + (n+1) H_2O \tag{2}$$
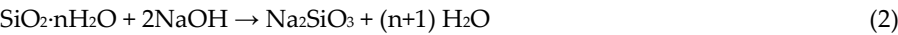
Acid–alkali treatment. For the experiment, 100 g of serpentinite waste (SP^0, the initial serpentinite sample) containing 25.75 g or 1.073 mol of Mg was used. According to the reaction equation (3):

$$Mg^{2+} + H_2SO_4 = MgSO_4 + 2H^+ \tag{3}$$

1.073 mol of H_2SO_4 was required for complete leaching of Mg from 100 g of SP^0.

A volume of 455 cm³ of a solution containing 1.073 mol of H_2SO_4 was placed in the reactor. Then, under stirring, 100.0 g of SP^0 was added, marking the start of the reaction time. Intense boiling was observed during the addition due to the exothermic nature of the reaction, resulting in the formation of a foamy mass. After 30 minutes, the suspension was filtered hot through a blue ribbon filter using vacuum suction.

The filtration time was 2 hours. The total volume of the obtained filtrate, including the washings, was 470 cm³, with a pH of 0.72.

The mass of the undissolved residue was 83.6 g. The filtrate was a clear, colorless liquid with a slightly yellowish tint. The residual amount of free sulfuric acid in the filtrate was determined by acid–base titration using 0.5 M NaOH solution.

The results are presented in Table 1.

Table 1. Consumption of H_2SO_4 during the leaching of Mg and accompanying elements from serpentinite waste (SP^0).

C₀(H_2SO_4), mol/L	Filtrate titration to pH = 7.5			$C_f(H_2SO_4)$, mol/L	$C_{cons}(H_2SO_4)$, mol/L
	pH of filtrate	V_filtrate, ml	V_NaOH, 0.5 M, ml		
1.073	0.72	10.00	27.90	0.36	0.64

Note: $C_0(H_2SO_4)$, $C_f(H_2SO_4)$ and $C_{cons}(H_2SO_4)$ denote the initial, final, and consumed concentrations of sulfuric acid, respectively.

The concentration of residual sulfuric acid after treatment was calculated using the following formula:

$$C_{1/2H_2SO_4} = C_{NaOH} \cdot V_{NaOH}/2 \cdot V_{H_2SO_4} \tag{4}$$

where: C_{NaOH} — concentration of the NaOH solution, mol/L; V_{NaOH} — volume of NaOH used for titration, mL; $V_{H_2SO_4}$ — volume of the sulfuric acid solution, mL.

The consumption of H_2SO_4 (%) was calculated using the following formula:

$$H_2SO_{4_{расход}} = \eta_{H_2SO_{4(consumed)}} \cdot 100/\eta_{H_2SO_{4(initial)}} \tag{5}$$

where: $\eta_{H_2SO_{4(consumed)}}$ – amount of sulfuric acid consumed, mol; $\eta_{H_2SO_{4(initial)}}$ – initial amount of sulfuric acid, mol.

The chemical composition of the filtrate obtained at 105°C and the insoluble residue was determined using a JSM-6490LV scanning electron microscope (JEOL, Japan) equipped with an INCA Energy 350 energy-dispersive microanalyzer.

Based on the chemical analysis results, the compositions of the filtrate and insoluble residue were determined, as well as the extraction degree of individual elements from the initial serpentinite waste SP^0. The distribution of elements in the filtrate and insoluble residue is presented in Table 2.

Table 2. Distribution of elements in the filtrate and insoluble residue after acid leaching of the initial serpentinite waste SP^0.

Element	In filtrate (wt.%)	In residue (wt.%)	Extraction (%)
Mg	64.8	35.2	64.8
Si	2.0	98.0	2.0
Fe	27.0	73.0	27.0
Mn	100.0	–	100.0
Cr	78.0	22.0	78.0
Ca	92.00	8.0	92.00
Al	66.0	34.0	66.0

Note: Values are expressed as percentages of the initial elemental content in the serpentinite waste (SP^0). The leaching was carried out using sulfuric acid at a concentration of 1.073 mol/L. Elemental composition was determined by scanning electron microscopy (SEM) with energy-dispersive X-ray spectroscopy (EDS) using a JSM-6490LV microscope (JEOL, Japan) equipped with an INCA Energy 350 microanalyzer.

According to Table 2, during the initial acid leaching of the serpentine waste SP^0 with sulfuric acid solution, a significant portion of magnesium, manganese, chromium, calcium, and aluminum (over 50%) is transferred into the sulfate solution.

At the same time, iron is only partially leached (27%), while silicon extraction is extremely low (2%).

The insoluble residue after leaching is substantially enriched in silicon (up to 98%) and iron (up to 73%).

The phase transformations occurring during acid leaching are illustrated by the X-ray diffraction patterns (Figure 1): the initial SP^0 (a) and the leached product SP^I (residue after acid treatment) (b). In diffractogram (b), the following phases were identified: chrysotile (SP^0), antigorite (AN) — $Mg_3Si_2O_5(OH)_4$, magnetite — Fe_2O_3, pyrope — $Mg_3Al_2[SiO_4]_3$, and almandine — $Fe_3Al_2[SiO_4]_3$. The main changes in the phase composition after acid treatment include the disappearance of brucite $[Mg(OH)_2]$ (BR) reflections at interplanar spacings d/n = 4.77; 2.365; 1.794 Å, and a reduction in the intensity of serpentinite (SP) peaks at d/n = 7.38; 3.661; 2.487; 1.53 Å and antigorite peaks at d/n = 7.30; 3.63; 2.52 Å.
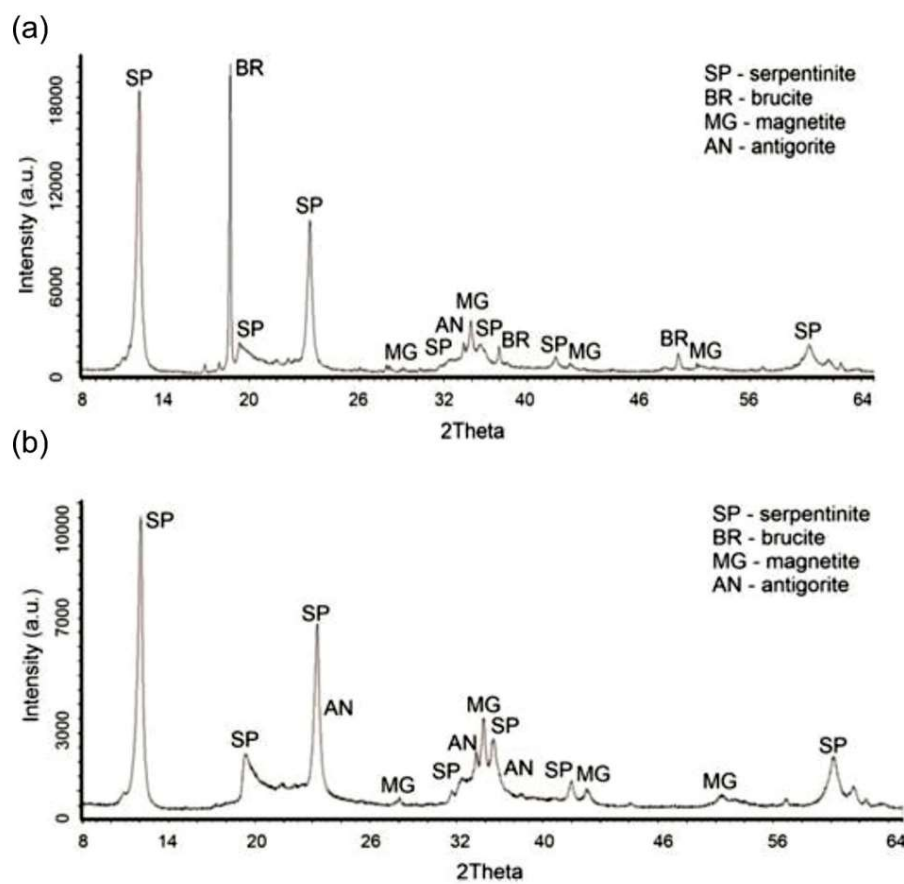
Figure 1. X-ray diffraction patterns of the initial serpentinite waste SP⁰ (a) and acid-treated sample SP¹ (b).

The phase transformation associated with the formation of amorphous silica is not observed in the SP¹ diffractogram.

However, its presence in the system is confirmed by the FTIR spectrum of the acid-insoluble residue (Figure 2).
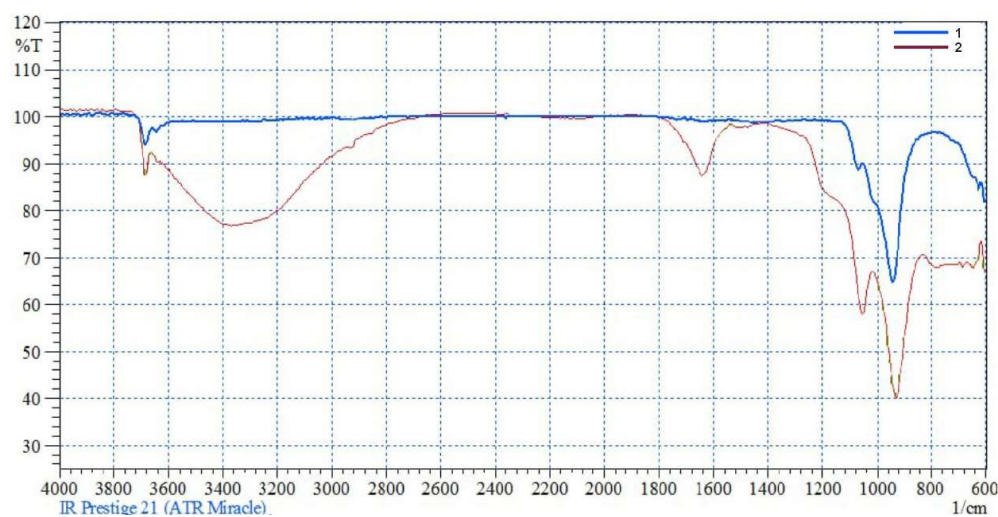

Figure 2. FTIR spectra of the initial sample SP⁰ (1) and the acid-insoluble residue (SP¹) (2) after acid treatment.

A shoulder characteristic of amorphous silica [10] at a stretching vibration frequency of v_{as}(Si–O–Si) = 1064 cm⁻¹ appears as a distinct peak.

This indicates the breakdown of the tetrahedral–octahedral layered structure of the serpentine crystal lattice and the formation of Si–OH hydroxyl groups on its surface.

As a result, an independent amorphous silica phase is formed in the system.

This assumption is further supported by X-ray diffraction analysis (Figure 3). The characteristic reflections of serpentine minerals (SP⁰) are suppressed due to the formation of $SiO_2 \cdot nH_2O$ after acid treatment (SP^I). These reflections reappear with increased intensity after alkaline treatment of the acid-insoluble residue (SP^{II}, residue after alkaline treatment), but their intensity decreases again after subsequent acid treatment of the alkaline residue (SP^{III}, residue after repeated acid treatment). The observed changes in the diffractograms during acid–alkaline processing of serpentinite indicate that the acid affects only the surface layer of the multilayer magnesium hydrosilicate.
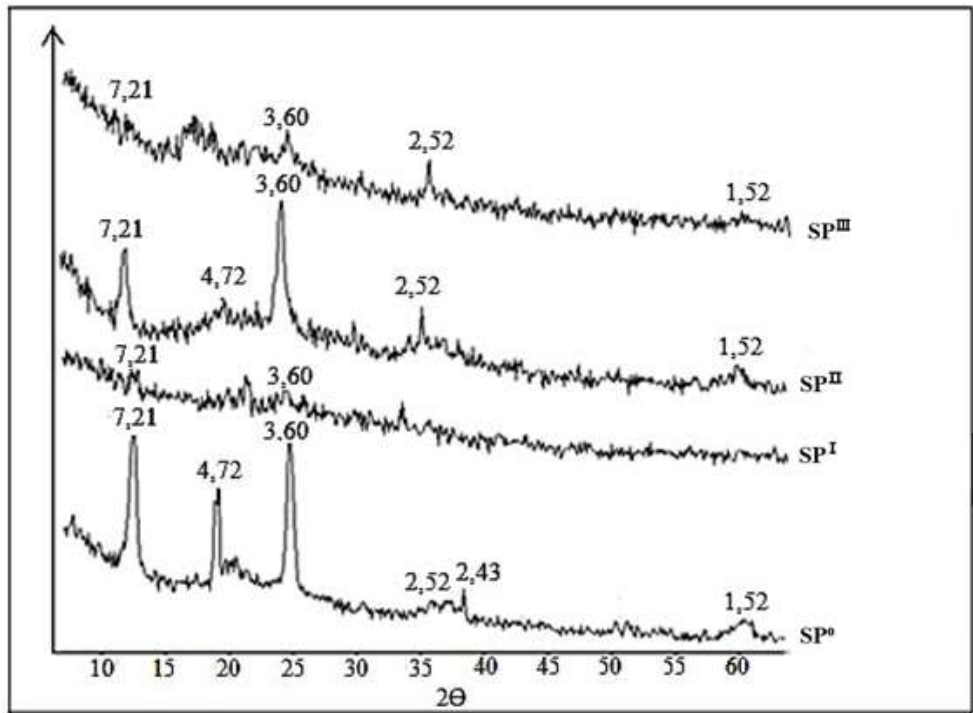

Figure 3. Diffractograms of samples: SP⁰ — initial serpentinite waste; SP^I — residue after acid treatment; SP^{II} — residue after alkaline treatment; SP^{III} — residue after repeated acid treatment, demonstrating phase composition changes on the surface during acid–alkaline processing of serpentinite.

Experimental studies conducted to verify this assumption were carried out as follows. The insoluble residue weighing 83.6 g (SP^I, obtained after acid treatment) was subjected to alkaline treatment (Stage 2). According to the elemental analysis of the insoluble residue (SP^I), formed after leaching of the initial SP⁰ with sulfuric acid solution, the following mass fractions were determined: Mg — 15.0%, Si — 21.2%, Fe — 3.0%, Cr — 0.19%, and S — 3.18%. Calculations based on the magnesium, silicon, and oxygen contents showed that the composition approximately corresponds to the formula: $1.25\ MgO \cdot 1.5\ SiO_2 \cdot 3H_2O$. The calculations performed to determine the stoichiometry of interaction between this composition and NaOH solution, as well as the conditions for silica precipitation, were carried out according to equations (1) and (2), presented in Table 3.

Table 3. Reactions and stoichiometric calculations for the interaction of the acid-insoluble residue (SP^I) with NaOH for silica precipitation.

Process	See equation	Molar mass, g/mol	Mass, g
Alkaline treatment of SP^I	Eq. (1): $1.25MgO \cdot 1.5SiO_2 \cdot 3H_2O + 3NaOH$ → $\mathbf{1.5Na_2SiO_3} + 1.25Mg(OH)_2 + 3.25H_2O$	194.00 + 120.00 → **183.00** + 72.5 + 58.5	83.60 + 51.70 → **78.86** + 31.24 + 25.21

| Acid treatment of silicate | Eq. (2): $Na_2SiO_3 + H_2SO_4 \rightarrow$ $SiO_2\downarrow + Na_2SO_4 + H_2O$ | $122.00 + 98.00 \rightarrow$ $60.00 + 142.00 +$ 18.00 | $78.86 + 63.35 \rightarrow$ $38.78 + 91.78 +$ 11.64 |

Note: The calculations are based on the average elemental composition of the acid-insoluble residue SP^I obtained after leaching with sulfuric acid. Equation (1) represents the alkaline decomposition of hydrated magnesium silicate and formation of sodium silicate. Equation (2) describes the precipitation of silica from sodium silicate using sulfuric acid.

According to Equation (1) (Table 3), 325 cm³ of 4.0 M NaOH solution (ϱ = 1.155 g/cm³) was used for the treatment.

A total of 83.6 g of the acid-insoluble residue (SP^I) was loaded into the reactor, followed by the addition of 325 cm³ of 4.0 M NaOH solution. The mixture was heated to boiling and stirred for 2 hours, after which it was filtered under vacuum. Filtration proceeded slowly but satisfactorily. The mass of the resulting insoluble residue (SP^I), obtained after alkaline leaching, washing, and drying at 105°C, was 36.6 g (SP^{II}). The elemental composition of SP^{II} (wt%) was as follows: Mg – 25.1; Si – 18.7; Fe – 9.64; Al – 0.27; Ca – 0.18; Cr – 0.17; O (calculated by difference) – 48.71. The combined volume of the filtrate and washing water was adjusted to 1000 cm³ using distilled water. The pH of the resulting solution was 11.46.

The filtrate was subsequently neutralized with 45% H_2SO_4 to pH 7.0 in accordance with Equation (2) (Table 3). As a result, a white fine-dispersed precipitate of silica formed and was separated by filtration. The mass of dry SiO_2, obtained after washing and drying the gel-like precipitate (230.0 g) from sodium sulfate and residual SO_4^{2-} (Ba^{2+} test), was 25.80 g. Elemental analysis of the resulting SiO_2 showed the following composition (wt%): Si – 42.03; Al – 0.23; Na – 0.75; O – 56.99.

The silica (SiO_2) yield was 95.78% based on the acidic residue (SP^I, 83.6 g), and 60.3% relative to the initial residue (SP^0).

Elemental analysis of the initial sample (SP^0), the acid-leached residue (SP^I), and the alkaline residue (SP^{II}) showed that after the two-step treatment SP^0 (acid and alkaline), the final residue SP^{II} became comparable in composition to the original SP^0 in terms of the main elements Mg and Si. In SP^0, the molar Mg/Si ratio was 1.68, while in SP^{II} it was 1.56.

These data indicate that after alkaline treatment, i.e., the removal of the silica layer from the surface of SP^I particles, the inner layers retain the serpentine structure [$Mg_3Si_2O_5(OH)_4$]. To confirm this assumption, the alkaline residue (SP^{II}, 36 g) was subjected to repeated acid leaching using a 2.0 M H_2SO_4 solution (stage 3). The resulting acid-insoluble residue (SP^{III}) was subsequently treated with alkali to obtain the alkaline residue (SP^{IV}). The experimental procedures applied at stages 3 (H_2SO_4 treatment) and 4 (NaOH treatment) were analogous to those used at stages 1 and 2. The obtained SP^{III} and SP^{IV} residues were also analyzed following the same approach as for SP^I and SP^{II}.

The summarized results of the elemental analysis of the insoluble residues after sequential acid–alkaline treatment (H_2SO_4 and NaOH) are presented in Table 4.

Table 4. Changes in the elemental composition (wt.%) of insoluble residues at different stages of sequential acid–alkaline treatment of serpentinite waste (SP) using H_2SO_4 and NaOH solutions.

Element	Initial SP^0	Stage 1 H_2SO_4 (SP^I)	Stage 2 NaOH (SP^{II})	Stage 3 H_2SO_4 (SP^{III})	Stage 4 NaOH (SP^{IV})
O	51.68	60.04	48.71	42.50	35.71
Mg	25.60	12.61	25.01	12.81	22.95
Al	0.47	0.19	0.27	n.d.	n.d.
Si	17.95	21.04	18.71	31.90	18.17
S	n.d.	4.85	n.d.	n.d.	n.d.
Ca	0.56	0.05	0.18	n.d.	n.d.
Cr	0.20	0.04	0.17	0.04	0.32

Mn	0.11	n.d.	n.d.	n.d.	n.d.
Fe	3.43	3.00	6.95	12.75	22.85
Σ (wt.%)	100.00	100.00	100.00	100.00	100.00
Conditional composition	$3MgO \cdot 2SiO_2$ $\cdot 2H_2O$	$1.25MgO \cdot 1.5SiO_2$ $\cdot 3H_2O$	$1.13MgO \cdot 0.72SiO_2$ $\cdot 0.72H_2O$	$0.53MgO \cdot 1.14SiO_2$ $\cdot H_2O$	$1.24MgO \cdot 0.84SiO_2$

Note: Elemental composition is given in weight percent (wt.%). n.d. – not detected. Conditional composition is estimated based on the main oxide components and assumed hydration level.

The analysis results of SP^{III} and SP^{IV} (Table 4) indicate that the dissolution mechanism of serpentinite in acids is most accurately described by the shrinking core model (Shrinking Core Model). The degree of dissolution is a function of the duration of the process, which may be prolonged depending on the activity of the serpentinite surface during its interaction with acid solutions.

Study of the properties of amorphous silica. The obtained silica contains no more than 1% impurities (0.75% Na + 0.25% Al) and approximately 8.0% adsorbed water, which corresponds to a composition of $SiO_2 \cdot 0.36H_2O$. The IR spectrum of silica with this composition is shown in Figure 4.
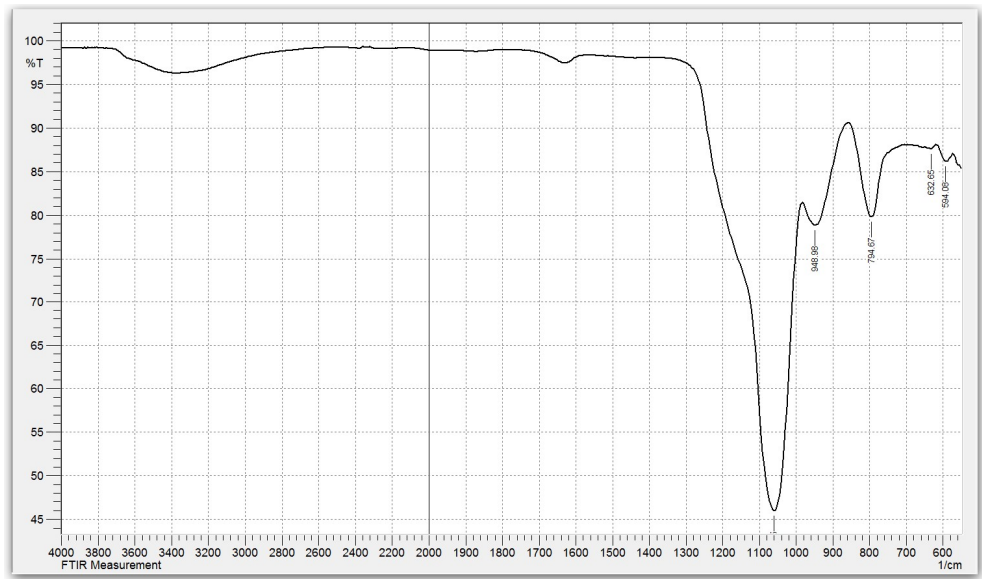

Figure 4. FTIR spectrum of amorphous silica ($SiO_2 \cdot 0.36H_2O$) obtained from the acid-insoluble residue of SP^I.

Characteristic absorption bands were observed at 3450 cm^{-1} (O–H stretching vibrations), 1630 cm^{-1} (H–O–H bending vibrations), and 1064 and 796 cm^{-1} (asymmetric and symmetric stretching vibrations of Si–O–Si bonds), confirming the amorphous structure of hydrated SiO_2 [11].

The obtained amorphous silica, containing more than 95.0% of the main SiO_2 component, can be used for various applications. Its specific surface area and adsorption properties, determined using the BET adsorption method, are presented in Figure 5.
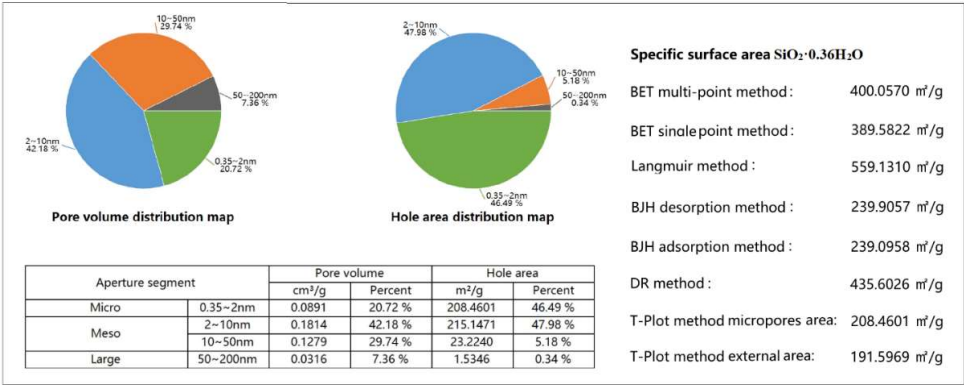
Figure 5. Specific surface area and adsorption characteristics of amorphous silica (SiO$_2$·0.36H$_2$O).

According to the pore volume distribution diagram, the SiO$_2$·0.36H$_2$O sample contains micropores with sizes ranging from 0.35 to 2 nm (20.72%), and mesopores in the ranges of 2–10 nm (42.18%) and 10–50 nm (29.74%), totaling 92.64%. The pore area distribution analysis shows that micropores contribute 46.49% of the surface area, while mesopores of 2–10 nm and 10–50 nm contribute 47.98 and 5.18%, respectively. Thus, the combined surface area contribution of micro- and mesopores reaches 99.65%, indicating a well-developed hierarchical porous structure.

The research results show that the amorphous silica obtained by the combined method has a high specific surface area and porous structure. According to the IUPAC classification, it is classified as mesoporous silica, which is recommended for use as an adsorbent, support, or catalyst matrix.

4. Conclusions

The combined acid–alkaline treatment method overcomes the limitations of traditional one-step approaches by enabling efficient magnesium dissolution and selective silicon extraction from serpentinite waste. The dissolution of the surface siliceous layer in the furnace, formed during acid treatment, facilitates further access of H$_3$O$^+$ ions to the inner mineral layers, which is consistent with the shrinking core model. The resulting amorphous silica is characterized by high purity (>95% SiO$_2$) and a well-developed mesoporous structure, making it a promising material for use as an adsorbent or catalyst support. The presented results demonstrate the efficiency of the combined acid–alkaline method and confirm its feasibility for developing new technological schemes for the processing of serpentinite and other magnesium-containing silicates.

Author Contributions: Conceptualization, A.A., Ch.Y.; methodology, A.A., Ch.Y.; software, E.D.; validation, A.I., K.A.; formal analysis, Ch.Y.; investigation, A.I., E.D.; resources, K.A., A.I.; data curation, E.D.; writing—original draft preparation, Ch.Y.; writing—review and editing, A.A.; visualization, K.A.; supervision, A.A.; project administration, A.A.; funding acquisition, A.A. All authors have read and agreed to the published version of the manuscript.

Institutional Review Board Statement: Not applicable. This study did not involve humans or animals.

Informed Consent Statement: Not applicable. This study did not involve human participants.

Data Availability Statement: The datasets generated and/or analysed during the current study are available from the corresponding author upon reasonable request.

Conflicts of Interest: The authors declare that they have no known competing interests.

References

1. Li, Y.; Zhang, X.; Wang, H. Acid leaching of magnesium from serpentine minerals. *J. Clean. Prod.* **2021,** *278*.
2. Zhou, X.; Liu, Y.; Hu, Z. Extraction of magnesium from serpentine using HCl. *Miner. Eng.* **2020,** *148*, 106217. [CrossRef]
3. Chen, L.; Zhao, J.; Wang, Y. Leaching of magnesium from serpentine with nitric acid. *Hydrometallurgy* **2022,** *208*, 105808. [CrossRef]
4. Rakhuba, V.; et al. Integrated processing of serpentine acid leachate using activated silicates. *Resour. Conserv. Recycl.* **2023,** *190*, 106731. [CrossRef]
5. Kurmangaliyev, K.A.; Ivanov, I.I.; Petrov, P.P. Hydrochemical processing of serpentine group minerals. *Vestn. KazNU. Ser. Chem.* **2019** [in Russian]
6. Musabekov, A.M. Purification of acidic solutions using thermally treated silicates. *Vestn. KazNU. Ser. Chem.* **2019.** [in Russian]
7. Auyeshov, A.; Arynov, K.; Yeskibayeva, Ch.; Dikanbayeva, A.; Auyeshov, D.; Raiymbekov, Y. Transformation of Silicate Ions into Silica under the Influence of Acid on the Structure of Serpentinite. *Molecules* **2024**, *29*, 2502. [CrossRef]
8. Yeskibayeva, Ch.; Auyeshov, A.; Arynov, K.; Dikanbayeva, A.; Satimbekova, A. Nature of serpentinite interactions with low- concentration sulfuric acid solutions. *Green Process. Synth.* **2024**, *13*, 20240034. [CrossRef]
9. Wang, L.; Liu, J.; Zhao, Y.; Zhang, X.; Wang, H.; He, S. Leaching kinetics of serpentine in sulphuric acid. *Hydrometallurgy* **2011**, *109(1–2)*, 141–146.
10. Chukin, G.D. *Surface Chemistry and Structure of Dispersed Silica*; Paladin Printa LLC: Moscow, Russia, 2008; p.172.
11. Matveev, V.A.; Zakharov, V.I.; Mayorov, A.V.; Kondratenko, T.V. Physicochemical properties of amorphous silicon dioxide isolated from nepheline. Russ. J. Inorg. Chem. **2011**, *56(3)*, 380–382. [in Russian]